corrosion and materials degradation

MDPI

Article

Development of Multifunctional CoAl Based Layered Double Hydroxide Protective Film on Aluminum Alloy

Muhammad Ahsan Iqbal [1,*], Humaira Asghar [2] and Michele Fedel [1]

[1] Department of Industrial Engineering, University of Trento, Via Sommarive 9, Povo, 38123 Trento, Italy; michele.fedel@unitn.it
[2] Department of Chemistry, University of Torino, Via Giuria 7, 10125 Torino, Italy; humaira.asghar@unito.it
* Correspondence: muhammadahsan.iqbal@unitn.it

Abstract: A protective CoAl-layered double hydroxide (LDH) thin film was developed directly on the aluminum substrate. Further, the low-surface-energy molecules (1H, 1H, 2H, 2H perfluorododecyl trichlorosilane) were incorporated inside the LDH network through an anion exchange mechanism to obtain a superhydrophobic CoAl-LDH surface. The developed films were characterized by scanning electron microscopy (SEM-EDS), X-ray diffraction (XRD), and Fourier transform infrared spectroscopy (FT-IR), and additional contact angle measurements were made to evaluate the superhydrophobicity of modified CoAl-LDHs against different solutions. The water contact angle (WCA) of the modified CoAl-LDH surface was observed to be about 153° and remained sufficiently stable after long-term immersion in NaCl solution. The effect of excessive ultrasonication on film structural variations and superhydrophobicity was also analyzed for outdoor applications. The high charge transfer resistance observed from the analysis of long-term electrochemical impedance spectroscopy (EIS) indicates the significant corrosion-resistance properties of the developed CoAl-LDHs. This research on protective CoAl-LDHs will bring insights into the understanding of new aspects of surface protection and implementation in many engineering applications.

Keywords: CoAl-LDHs; superhydrophobic; self-cleaning; EIS

Citation: Iqbal, M.A.; Asghar, H.; Fedel, M. Development of Multifunctional CoAl Based Layered Double Hydroxide Protective Film on Aluminum Alloy. *Corros. Mater. Degrad.* **2021**, *2*, 708–720. https://doi.org/10.3390/cmd2040038

Academic Editors: Väino Sammelselg and Luigi Calabrese

Received: 12 October 2021
Accepted: 29 November 2021
Published: 1 December 2021

1. Introduction

Layered double hydroxides (LDHs), a fascinating two-dimensional material system, have gained an attractive class of anionic clays where diverse functional properties, i.e., wide anion exchangeability, environmental suitability, adsorption capacity, wide compositional variations, controllable bandgap energy, photocatalysis, and electrical properties, are highly discussed [1–4]. These make LDHs an attractive choice to investigate in various fields, such as adsorption [5], drug delivery [6], catalysis [7], supercapacitors [8], and photocatalytic environmental science [9]. In coating engineering, layered double hydroxide-based systems are considered a smart solution to develop a multifunctional protective coating system for light metallic alloys [10–15]. The main constituents of LDHs are metal cations layers (divalent source, i.e., Mg^{2+}, Zn^{2+}, Ca^{2+}, and Ni^{2+}, etc., and trivalent source, i.e., Fe^{3+}, Al^{3+}, Cr^{3+}, etc.) in the stacking layers and intercalated anionic species.

Superhydrophobic LDH surfaces have gained a great deal of attention, where a range of unique interests have been developed in oil–water separation [16], self-cleaning [11], anti-icing [17], water repellency [18], and anti-corrosion properties [19–22]. The concept of self-cleaning corrosion-resistant coatings can be divided into two categories: (a) superhydrophobic surfaces and (b) photocatalytic materials. The former coatings clean themselves by rolling water droplets that carry away dirt contaminations, and the latter coating approach chemically breaks down the absorbed dirt particles in the sunlight and results in a clean surface [23]. The superhydrophobic self-cleaning characteristics and improved corrosion-resistance properties of LDHs on aluminum surfaces are already well reported by various research groups [11,19,24,25]. However, the protective performance of

photocatalytic LDH materials has not yet been investigated to the best of our knowledge. Cobalt-based LDH materials exhibit unique optical properties, showing discrete absorption lines in the visible spectral range and have been investigated as photocatalyst materials for Fenton reactions [26,27] and in the photodecomposition of complex organic molecules such as methyl orange [28], nitrobenzene [29], rhodamine B, and acid red G [30]. Therefore, it is of considerable interest to learn how to control the preparation of cobalt-based layered double hydroxide directly on the metallic surface, where the conductive surface may facilitate the efficient transportation of photogenerated charges. In order to use CoAl-LDH-based anti-corrosion materials, it is necessary to discover the approach for easy synthesis directly on the substrate, and understand the corrosion-resistance properties, anion-exchange properties, and self-cleaning characteristics. To the authors' knowledge, no brief reports are available on the synthesis of CoAl-LDHs on a metallic surface or fundamental corrosion-resistance properties. The idea of the present study is to develop cobalt-based layered double hydroxide directly on an aluminum substrate to understand its long-term corrosion-resistance properties and subsequently modify it with perfluorododecyl trichlorosilane to develop superhydrophobic CoAl-LDHs to achieve long-term stability and self-cleaning characteristics. Additional chemical and mechanical stabilities are also evaluated.

2. Materials and Synthesis

2.1. Pretreatment

The AA6082 substrate constituted 0.70–1.30% silicon, 0.40–1.00% manganese, 0.60–1.20% magnesium, 0.50% iron, 0.10% copper, and a balanced percentage of aluminum. The substrate, with a 3.14 cm^2 surface area, was initially ground with 400, 1200, 2400, and 4000 SiC grit-size papers, and was rinsed with distilled water. The specimens were ultrasonically cleaned with ethanol for 10 min and were etched with 0.1 M aqueous NaOH solution for 1 min.

2.2. Synthesis of CoAl-LDHs

To develop CoAl-LDHs, initially, 0.02 M Co $(NO_3)_2{\cdot}6H_2O$ (≥99%, Sigma Aldrich, St. Louis, MI, USA) solution was prepared at a pH of 6 by the drop-wise addition of 1 M NaOH solution and transferred to a 1000 mL Teflon-lined autoclave. The solution was purged with nitrogen gas for 10 min to remove the absorbed gases. The pretreated AA6082 (3.14 cm^2 surface area) was placed in the above solution (800 mL) and the autoclave was placed at 120 °C for 24 h in an oven. The obtained CoAl-LDHs were washed with distilled water and dried at room temperature. To develop superhydrophobic CoAl-LDH, the CoAl-LDH specimen was immersed in 1H, 1H, 2H, 2H perfluorododecyl trichlorosilane solution/$CF_3(CF_2)_9CH_2CH_2SiCl_3$ (≥97%, Sigma Aldrich) for 2 h at 40 °C. The PFDTS solution was prepared by adding 0.1 g PFDTS to 200 mL ethanol [11]. The obtained specimen is referred to as CoAl-LDHs-S for simplicity. Figure 1 shows the optical images of the developed CoAl-LDH specimens. It is reported that the surface colors of the CoAl-LDHs were distinct due to the complex cobalt chemistry and based on the specific oxidation state of cobalt ions, where the Co/Al ratio made an influential impact on the appearance of a specific color, i.e., blue, pink, greyish brown, and yellowish brown. The obtained yellowish-brown color in this work (Figure 1) is in good accordance with the reported study, where the oxidative reaction of $Co(OH)_2$ resulted in the cobalt oxide/hydroxide compound (CoO(OH)) (Equation (1)) with a hexagonal layered structure and resulted in a yellowish-brown color at a molar ratio of Co/Al = 5 [31,32].

$$4[Co(OH)_2] + O_2 \rightleftharpoons 4[CoO(OH)] + 2H_2O \quad (1)$$

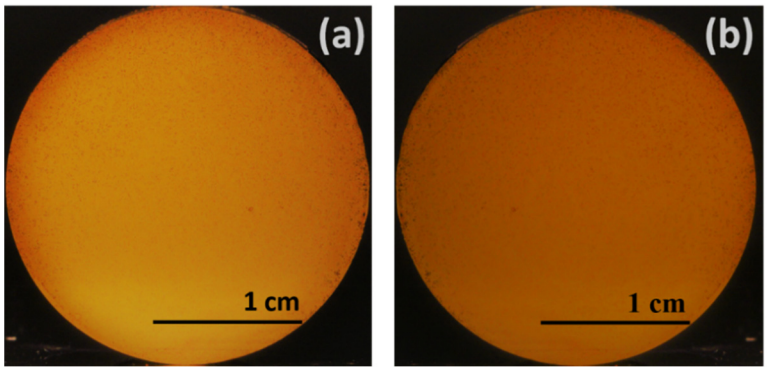

Figure 1. Optical images of as-prepared (**a**) CoAl-LDHs and (**b**) CoAl-LDHs-S.

3. Characterization

The surface morphology and the elemental composition of the developed LDH specimens were studied by scanning electron microscopy/JEOL-JSMIT300 equipped with an EDS detector. X-ray diffraction (X'Pert High Score diffractometer, Rigaku, Tokyo, Japan /30 kV, 10 mA, and Cu Kα radiation) was used to analyze the crystalline structure. Attenuated total reflection Fourier transform infrared spectroscopy (Varian 4100 FTIR Excalibur Series instrument (Varian, Santa Clara, CA, USA), spectra were obtained in the range of 525–4000 cm^{-1} at a resolution of 4 cm^{-1}. The static contact angle (CA) measurements were made by acquiring the picture of liquid drops on the surface. The mechanical stability of the superhydrophobicity was estimated under ultrasonication (100 W, 99% amplitude) for 30 min and CAs were recorded after ultrasonication. The electrochemical impedance spectroscopy (EIS) measurement was taken by using Princeton Applied Research "Parstat 2273", (Ametek, Berwyn, PA, USA) Potentiostat/Galvanostat/FRA equipment with an Ag/AgCl (3.5 M KCl, +0.205 V vs. SHE) reference electrode and platinum as a counter electrode. The impedance measurements were taken with an amplitude of 10 mV at a frequency range of 0.01 Hz to 100 kHz.

4. Experimental Results

The SEM images of developed CoAl-LDH thin films are shown in Figure 2, where a nest-like LDH microstructure uniformly grew perpendicular on the aluminum substrate. After modification with PFDTS, the platelet morphology of CoAl-LDHs became more compact and transformed into a packed flower-like structure possibly due to the induced stress of PFDTS in the LDH network, which could then be relaxed by the formation of a disordered packed surface. The platelet structure in the case of CoAl-LDHs-S remained unchanged except that the thickness was found to increase after modification. The EDS results (Figure 3) show that CoAl-LDHs were mainly composed of Co, Al, oxygen, and nitrogen. After treatment with the PFDTS solution, the content of cobalt and oxygen was reduced in CoAl-LDHs, and the contents of fluorides, chlorides, and carbon were introduced in the CoAl-LDH composition. The Co element after modification reduced from 25.61% to 14.97% along with the further appearance of fluoride (23.9%), chloride (2.7%), and carbon (23.2%) contents, indicating that PFDTS was successfully adsorbed/bonded with the CoAl-LDHs. The atomic ratio of Co/Al was 4.57 in the case of CoAl-LDHs, which changed to 3.55 for CoAl-LDHs-S. These results support the explanation of morphology variations after modification of CoAl-LDHs with PFDTS. The thickness of the CoAl-LDH film was approximately 9.4 ± 0.8 μm, which after modification increased a bit, with an average value of 10.5 ± 0.7 μm.

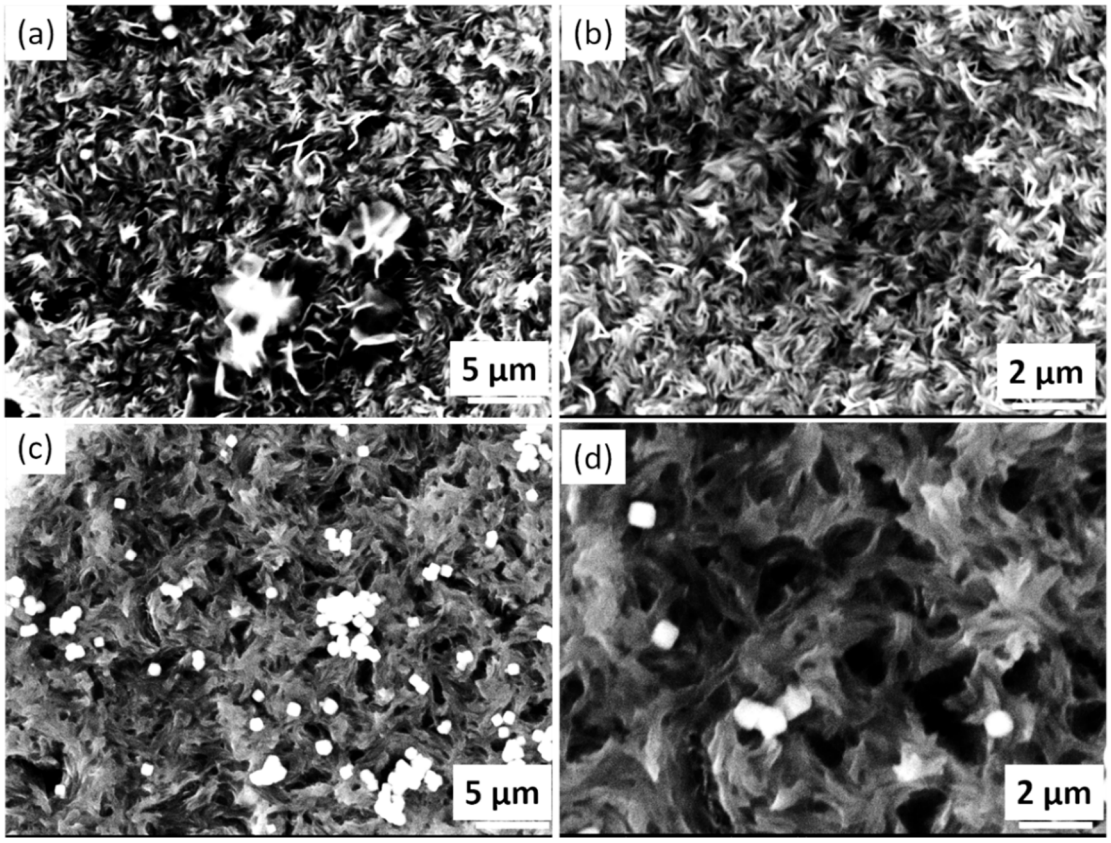

Figure 2. SEM images of thin films: (**a**,**b**) CoAl-LDHs, (**c**,**d**) CoAl-LDHs-S.

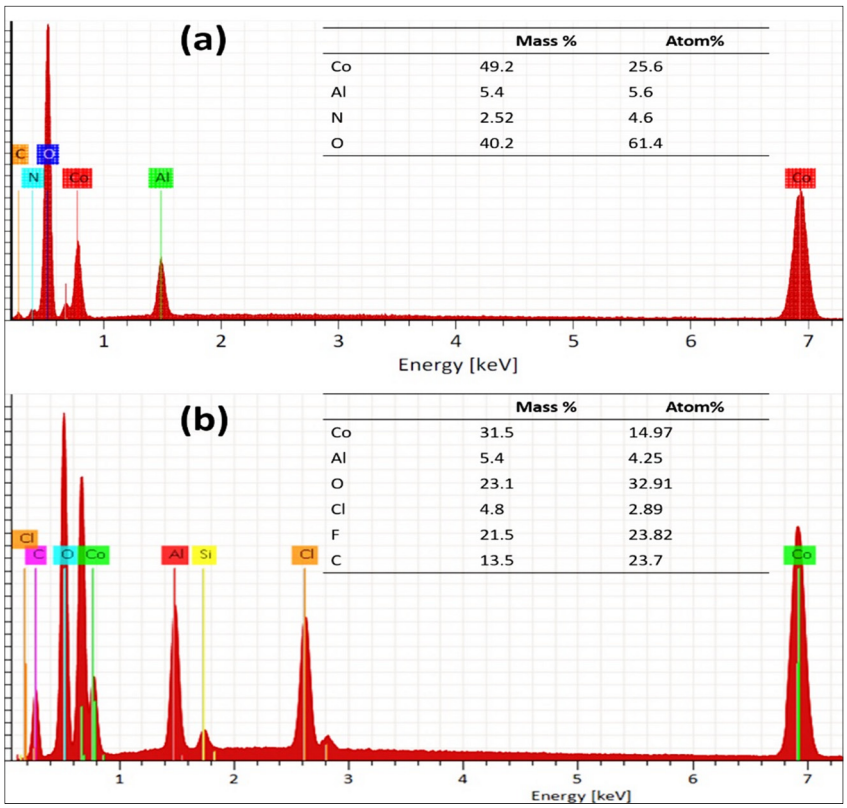

Figure 3. EDS analysis and corresponding elemental compositions: (**a**) CoAl-LDHs and (**b**) CoAl-LDHs-S.

XRD patterns (Figure 4) of CoAl-LDHs showed distinct peaks of LDHs at 11°, 23°, 35°, 61°, and 63°, which corresponds to 003, 006, 012, 110, and 113 diffraction planes, indicating the typical LDH structures. The calculated basal spacing (0.80 nm) of CoAl-LDHs at position 003 by using brag law confirmed the presence of nitrates inside the LDHs. The diffraction line positions of CoAl-LDHs-S remained almost the same as those of CoAl-LDHs; however, a slight shift of the 003 diffraction line towards the left side was observed, which indicates the possible intercalation of PFDTS in CoAl-LDHs. The diffraction line appeared at around 20° and 37° of developed CoAl-LDHs, belonging to the reflection lines of the CoO(OH), whereas $Co(OH)_2$ was confirmed by the 32° diffraction line position. PFDTS was hydrolyzed in absolute ethanol to obtain $CF_3(CF_2)_9CH_2CH_2Si(O^-)_3$ groups, which were incorporated in CoAl-LDHs. When PFDTS was added to ethanol, a hydrolysis reaction of PFDTS occurred. Si-OH groups could be obtained due to the hydrolysis of the three Si-Cl groups of PFDTS [33]. Thus, it could induce hydrogen bond formation between Si-OH groups and -OH groups of LDH. Meanwhile, their d values were higher than those of unmodified Co/Al LDH. This may have been due to the anion exchange reaction between PFDTS and LDH, which led to the increase in the interlayer distance and indicated the functionalization of CoAl-LDHs by long-chain PFDTS.

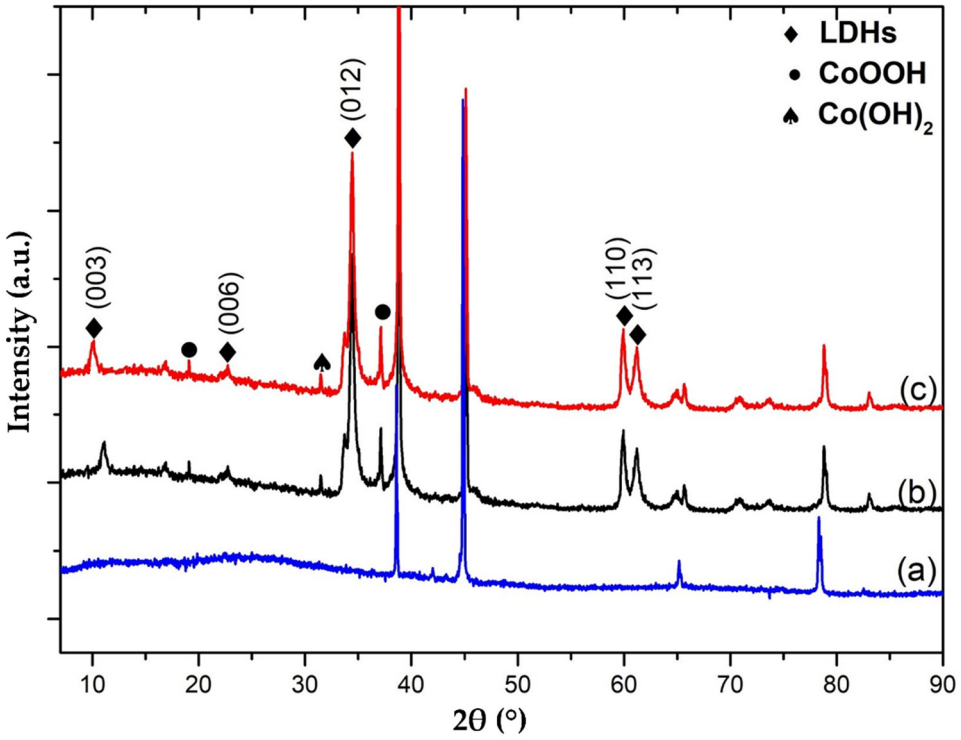

Figure 4. The XRD spectra of developed CoAl-LDH films: (**a**) AA6082, (**b**) CoAl-LDHs, (**c**) modified CoAl-LDHs.

The ATR-FTIR spectra of CoAl-LDHs (coating scraped from the surface) demonstrated the traditional absorption peaks of LDH-based systems (Figure 5), where the H-O-H stretching vibration of water molecules was found to be in the range of 3000 to 3600 cm^{-1}, whereas the peak at 1627 to 1633 cm^{-1} corresponded to the bending vibration of interlayer water molecules [34]. In addition, the peak observed at 1380 cm^{-1} was assigned to the asymmetric stretching bond of intercalated NO_3^- [35]. Furthermore, Al-OH structuring was confirmed by the peaks at 749 and 1202 cm^{-1} [36] and metal-oxygen bonds by the absorption peak of 552 cm^{-1} [37].

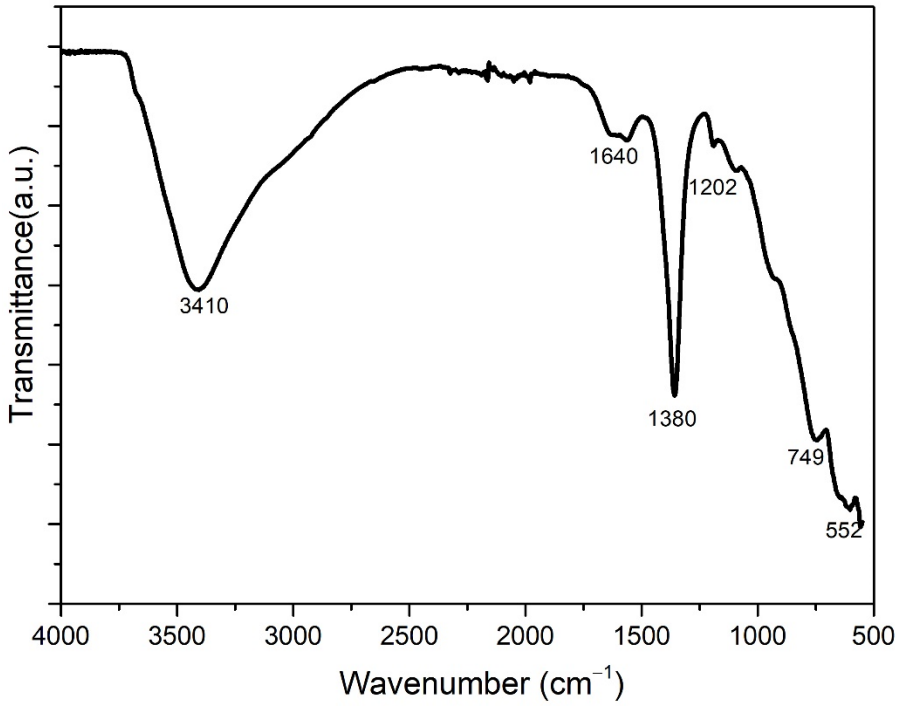

Figure 5. ATR-FTIR analysis of CoAl-LDHs.

To understand the self-cleaning characteristics of superhydrophobic CoAl-LDHs against the variety of common household items, contact angle measurements were analyzed. The optical images of the droplets are shown in Figure 6. It can be seen that water, NaOH, NaCl, coffee, and graphite solution droplets stood almost spherical on the CoAl-LDHs-S surface. However, acid droplets spread with a comparatively lesser contact angle on the surface. The dense Si-O-Si network within modified CoAl-LDHs coating played a good synergistic effect to improve the compactness and hydrophobicity. The hydrophobic coatings with fluoroalkane groups on the LDH micro-scale hierarchical structure were beneficial to create superhydrophobicity and improved barrier properties [38].

Mechanical stability is another parameter that needs to be evaluated for outdoor applications since physical damage is inevitable, and it is necessary to investigate the effect of surface distortions on surface wettability and structural stability. Therefore, the mechanical durability was taken into consideration by the ultrasonic treatment of CoAl-LDHs-S for 30 min, and the superhydrophobicity after structural distortions was analyzed. The SEM images of the samples after ultrasonication are shown in Figure 7. It is clear that the LDH structure after the ultrasonication process remained intact, and except for a few LDH curvy plate distortions, no other dominant defects were observed. However, CoAl-LDHs-S morphology showed more intactness than CoAl-LDHs. Figure 8 demonstrates the optical images of liquid drops of water, 1 M NaOH, and 0.1 M NaCl solution on CoAl-LDHs-S. It was found that the contact angles of the liquid drop were 147.2°, 144.3°, and 141.3° for water, 1 M NaOH, and 0.1 M NaCl solution, respectively. The observed contact angles indicated a slight recession of the superhydrophobicity; however, this suggests the film's stability and sustainability of superhydrophobicity after abrasive damage.

The EIS spectra measured in 0.1 M NaCl solution after 30 min are represented in Figure 9. The impedance modulus at low frequency (0.01 Hz, $|Z|_{0.01}$) is a rough estimation of the overall corrosion resistance properties of the developed CoAl-LDHs specimens. CoAl-LDHs-S showed $|Z|_{0.01}$ values around more than one order of magnitude higher than the CoAl-LDH, and about four orders of magnitude higher than the bare AA6082 substrate. At $|Z|_{0.01}$, CoAl-LDHs and CoAl-LDHs-S demonstrated around a 10^7 Ω·cm^2 and $10^{8.5}$ Ω·cm^2 impedance modulus ($|Z|_{0.01}$), respectively, which is significantly higher than the aluminum substrate (10^5 Ω·cm^2), as shown in Figure 9I. The CoAl-LDHs-S depicted

higher impedance values in the middle–high frequency range as well, suggesting better resistance of the upper layer and a reduced corrosion rate. CoAl-LDHs showed significant corrosion-resistance properties, better active and passive corrosion protection, and long-term stability against corrosive species. The considerable corrosion resistance of cobalt-based LDHs can be explained by the following: (i) the barrier effect of the compact LDH layer, and (ii) the ion-exchange mechanism of CoAl-LDHs, which held the corrosive species inside the interlayers of LDHs and did not allow them to contact the underlying aluminum substrate. The modification of CoAl-LDHs with PFDTS was found to additionally increase the low-frequency modulus considerably. EIS phase angle plots (Figure 9II) of the CoAl-LDH-based system showed mainly two time constants, one in a medium-frequency range that corresponds to the inner barrier layer, and another at a high–medium-frequency range that corresponds to the outer porous layer. The CoAl-LDHs-S in that sense showed a superior inner barrier layer than the CoAl-LDHs, which explains the concept of superhydrophobicity and improved corrosion-resistance properties well. Considering the high-frequency range of the phase angle diagram (Figure 9II), CoAl-LDHs-S showed around a 15° larger phase angle than CoAl-LDH, and a phase angle around 65° higher than that of the aluminum substrate, which demonstrates the superior anticorrosion characteristics of CoAl-LDH-based systems.

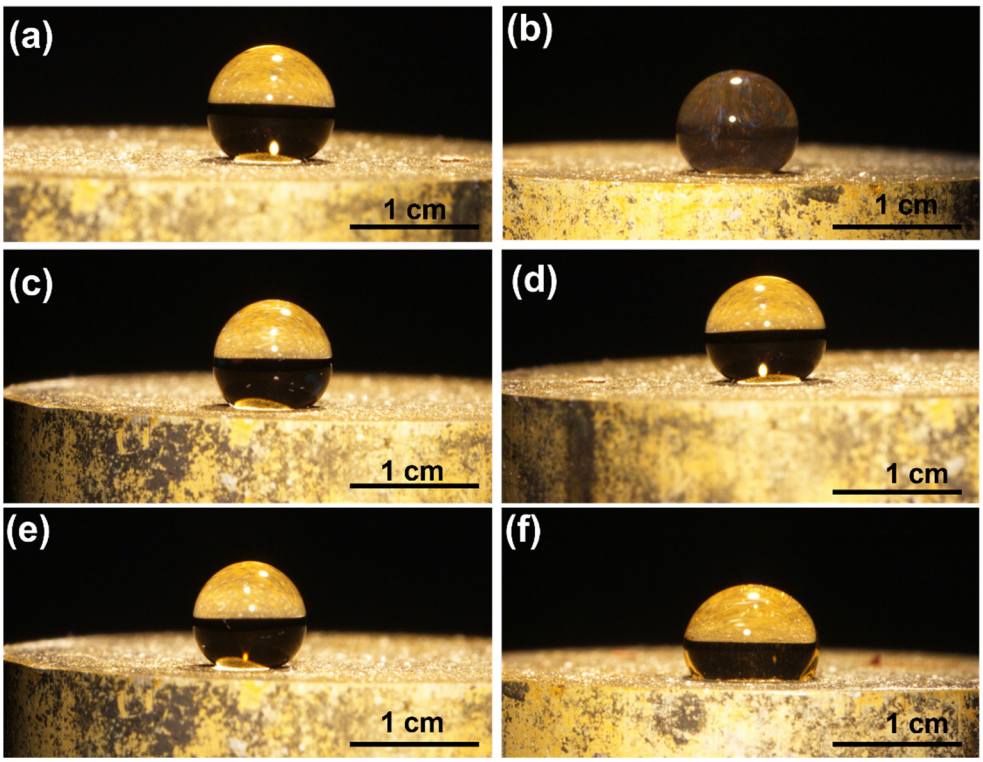

Figure 6. Digital photos of different liquid droplets on the CoAl-LDHs-S surface: (**a**) water (**b**) graphite solution, (**c**) 1 M NaOH, (**d**) coffee, (**e**) 0.1 M NaCl, (**f**) acidic solution (pH ~ 3).

To understand the long-term stability, the impedance modulus of both developed CoAl-LDHs systems were evaluated from 24 h to 720 h in 0.1 M NaCl solution (Figure 10). It was observed that the $|Z|_{0.01}$ value of CoAl-LDH-S was reduced from 10^8 to about $10^{7.1}$ $\Omega \cdot cm^2$ after 720 h, and in the case of CoAl-LDH, it was reduced from $10^{7.2}$ to about 10^6 $\Omega \cdot cm^2$. However, the decline rate for both cases almost remained the same, wherein in both cases a $|Z|_{0.01}$ decrease of an order of around $10^{1.2}$ was found to occur. This defined the performance of the CoAl-LDHs network and verified the concept of the utilization of CoAl-LDHs as another class of anti-corrosion LDH system. The findings describe the higher stability of CoAl-LDHs-S, where superhydrophobicity induces additional corrosion-resistance properties. The strong passive and active protection were found to develop the

compactness and integrity of LDHs, which is significant for delaying the corrosion process and is a powerful approach to enhancing anti-corrosion behavior [39]. Figure 11 shows the declining rate of $\log |Z|_{0.01}$ $\Omega \cdot cm^2$ from 1 to 720 h, where the CoAl-LDHs and CoAl-LDHs-S showed almost the same declining rate, as explained above and demonstrating the significant corrosion resistance of LDHs. The declining impedance modulus rate of as-prepared CoAl-LDHs was much slower after a long immersion time than the other reported LDH systems, i.e., MgAl-LDHs, CeMgAl-LDHs, LiAl-LDHs, and NiAl-LDHs [40–43].

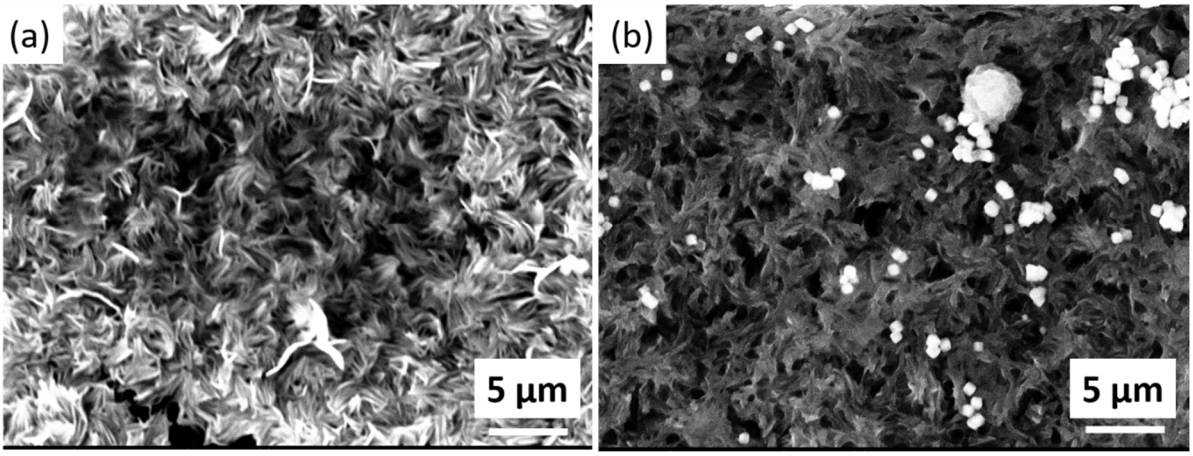

Figure 7. SEM images after ultrasonication: (**a**) CoAl-LDHs, (**b**) CoAl-LDHs-S.

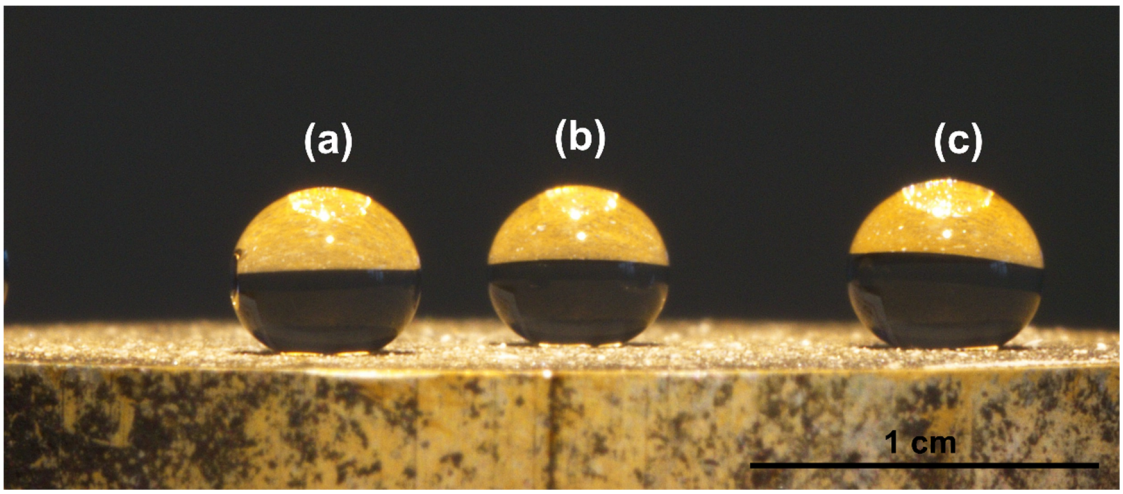

Figure 8. Optical images of liquid droplets on the surface of CoAl-LDHs-S after ultrasonication treatment: (**a**) water, (**b**) 0.1 M NaCl, and (**c**) 1 M NaOH.

Due to higher surface roughness, the CoAl-LDHs-S formed a possible air film on the surface, which acted an additional barrier layer for the LDH thin film in contact the corrosive solution [19]. For practical applications, long-term superhydrophobicity plays an important role, so the change of water contact angle measurements was monitored while in continuous contact with 0.1 M NaCl solution from 1 h to 720 h, as shown in Figure 12. The average contact angle decreased from 153° to 142° after immersion in 0.1 M NaCl solution in a time frame of 24 h to 720 h (Figure 12a,b). The declining rate of 11° after 720 h immersion confirms the long-term stability of the superhydrophobic surface against the corrosive solution. The CoAl-LDHs-S in that sense consisted of four parts: (a) air film, (b) LDH layers, (c) intercalated nitrates/PFDTS species, and (d) LDH/substrate interface. The air film, dense LDH/substrate interface, and LDH layers between them constituted all of the protective layers, all of which contributed to impeding the invasion of water

molecules and chlorides. In summary, it can be concluded that the CoAl-LDHs-S can provide efficient protection for the aluminum substrate, and CoAl-LDHs also showed significant corrosion protection after 720 h of analysis.

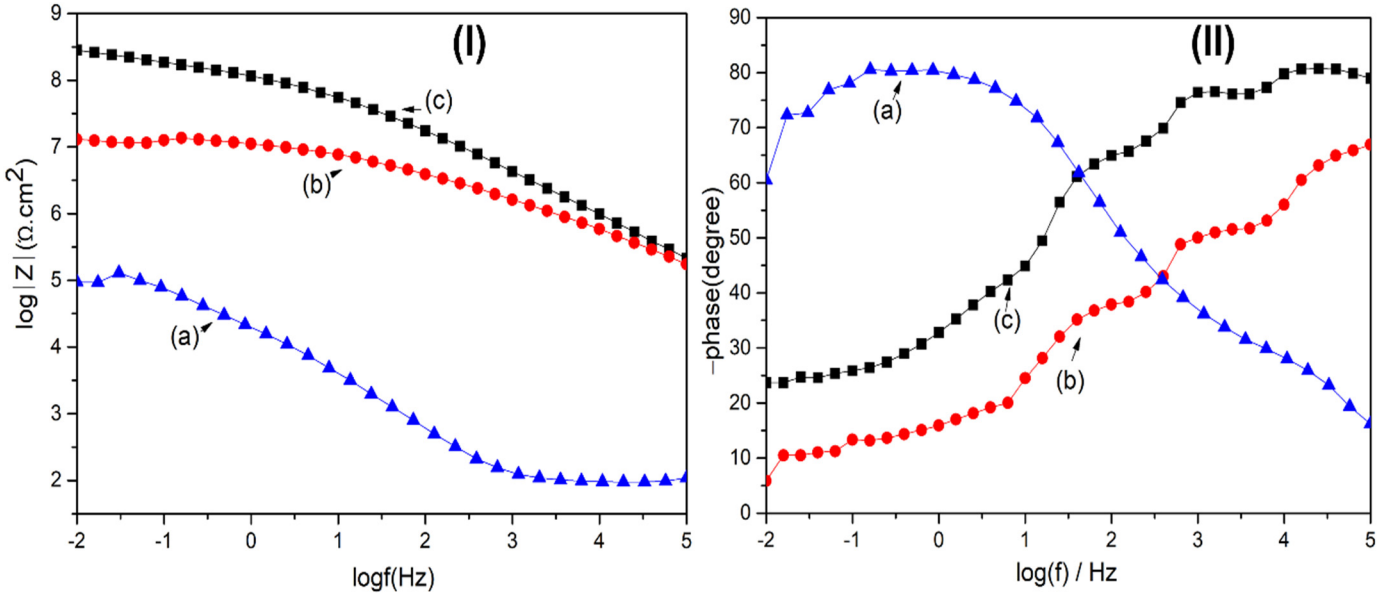

Figure 9. Bode plots and phase angle plots: (**a**) AA6082 substrate, (**b**) CoAl-LDHs, and (**c**) CoAl-LDHs-S.

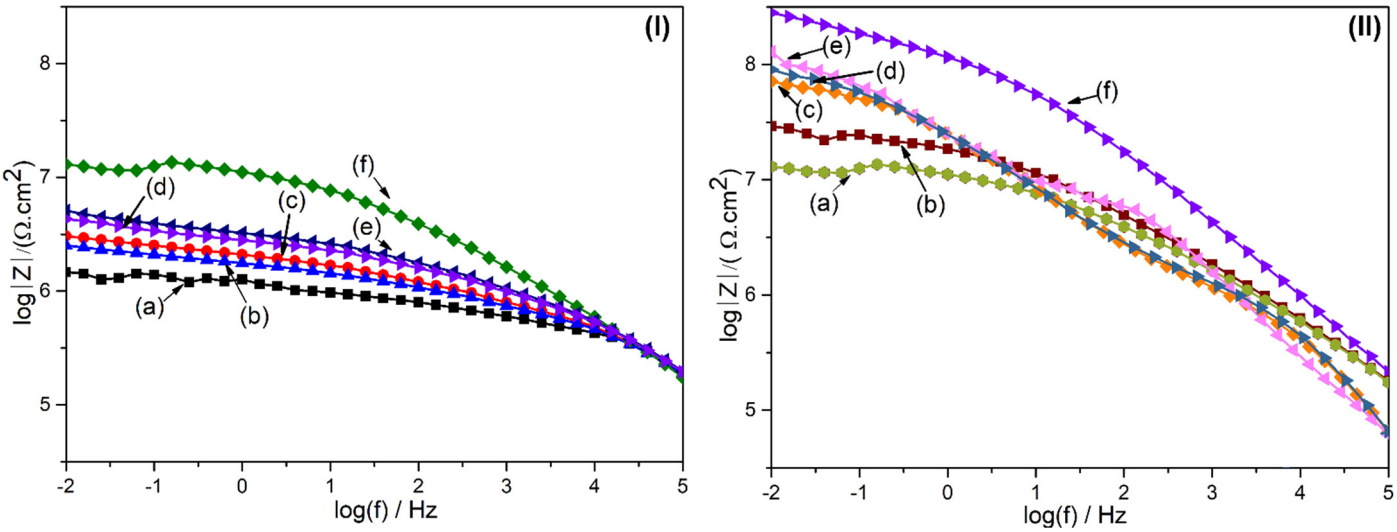

Figure 10. Bode plots of (**I**) CoAl-LDHs and (**II**) CoAl-LDHs-S from 24 to 720 h: (**a**) 720 h, (**b**) 504 h, (**c**) 336 h, (**d**) 168 h, (**e**) 72 h, and (**f**) 24 h.

The EIS results were also good following the visual observation of the immersed samples, as shown in Figure 13. The optical photos were taken after the 720 h EIS measurements in 0.1 M NaCl solution. The bare aluminum sample was found to corrode badly with a thick layer of corrosion products, whereas the CoAl LDH and CoAl-LDHs-S films almost sustained the original structure and no clear corrosion products were observed. The formation of insulative air film and the presence of long-chain PFDTS inside LDHs network prevented electron transfer and the attack of chlorides and water molecules at the substrate. The stability of contact angle measurements of CoAl-LDHs-S after long-term immersion in NaCl solution was also in good agreement with the optical photos of LDHs (Figure 13), where comparatively no sign of corrosion products or pitting was observed. The aluminum

corrosion was retarded by the formation of LDHs, whereas the sample of CoAl-LDHs-S presented a more significant $|Z|_{0.01}$ value compared to CoAl-LDHs, which exhibited active anticorrosion performance of CoAl-LDHs-S. The CoAl-LDHs-S characteristics make an attractive option for anticorrosion thin films; however the photocatalytic properties for the destruction of organic specks of dirt also need to be address.

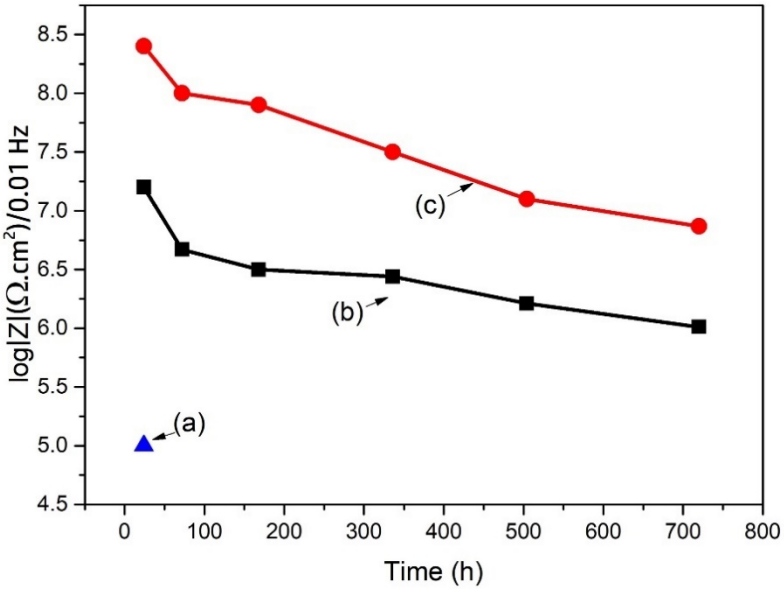

Figure 11. Impedance modulus at 0.01 Hz against various immersion times: (**a**) AA6082, (**b**) CoAl-LDHs, and (**c**) CoAl-LDHs-S.

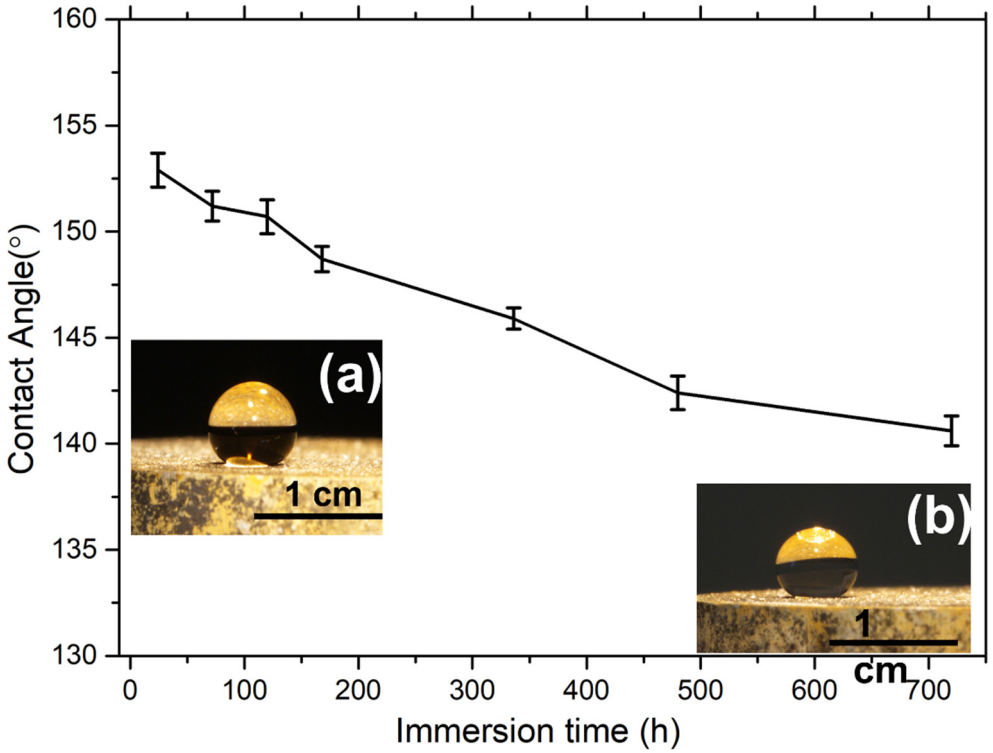

Figure 12. Contact angle of CoAl-LDHs-S against immersion time in 0.1 M NaCl solution.

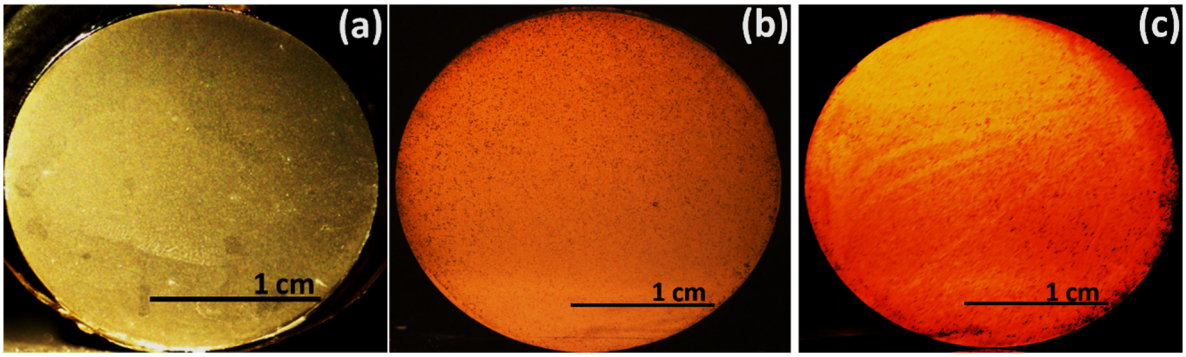

Figure 13. The specimen surfaces after 720 h EIS analysis: (**a**) aluminum AA6082, (**b**) CoAl-LDHs, and (**c**) CoAl-LDHs-S.

5. Conclusions

CoAl-LDHs thin films were successfully developed on an aluminum AA6082 surface and were further utilized to design superhydrophobic nanocomposite thin film by embedding PFDTS inside an LDH structure. Based on the impedance modulus, CoAl-LDHs and CoAl-LDHs-S coatings showed almost the same reduction rate of $|Z|_{0.01}$; however, overall, CoAl-LDHs-S showed superior corrosion-resistance properties. The CoAl-LDHs-S showed an average WCA of 153° and remained stable upon long-term contact with NaCl solution, as well as after vigorous ultrasonication. The superhydrophobic surface also showed sufficient contact angles against the common household solution, suggesting the robustness of the CoAl-LDHs-S surface against chemical damage. The developed coatings demonstrated significant corrosion protection and can open windows for new applications.

Author Contributions: Conceptualization, M.A.I. and M.F., methodology, H.A. and M.A.I.; validation, M.F. and M.A.I.; formal analysis, M.A.I.; investigation, M.A.I. and H.A.; data curation, M.A.I. and H.A.; writing—original draft preparation, M.A.I.; writing—review and editing, M.F.; visualization, H.A.; supervision, M.F. All authors have read and agreed to the published version of the manuscript.

Funding: This research received no external funding.

Institutional Review Board Statement: Not applicable.

Informed Consent Statement: Not applicable.

Data Availability Statement: Not applicable.

Conflicts of Interest: The authors declare no conflict of interest.

References

1. Iqbal, M.A.; Sun, L.; Barrett, A.T.; Fedel, M. Layered double hydroxide protective films developed on aluminum and aluminum alloys: Synthetic methods and anti-corrosion mechanisms. *Coatings* **2020**, *10*, 428. [CrossRef]
2. Wu, M.J.; Wu, J.Z.; Zhang, J.; Chen, H.; Zhou, J.Z.; Qian, G.R.; Xu, Z.P. (Gordon); Du, Z.; Rao, Q.L. A review on fabricating heterostructures from layered double hydroxides for enhanced photocatalytic activities. *Catal. Sci. Technol.* **2018**, *8*, 1207–1228. [CrossRef]
3. Zheludkevich, M.; Poznyak, S.; Rodrigues, L.; Raps, D.; Hack, T.; Dick, L.F.P.; Nunes, T.; Ferreira, M. Active protection coatings with layered double hydroxide nanocontainers of corrosion inhibitor. *Corros. Sci.* **2010**, *52*, 602–611. [CrossRef]
4. Guo, X.; Zhang, F.; Evans, D.G.; Duan, X. Layered double hydroxide films: Synthesis, properties and applications. *Chem. Commun.* **2010**, *46*, 5197–5210. [CrossRef] [PubMed]
5. Iqbal, M.A.; Asghar, H.; Fedel, M. Sorption of As(V) from aqueous solution using in situ growth MgAl–NO_3 layered double hydroxide thin film developed on AA6082. *SN Appl. Sci.* **2019**, *1*, 666. [CrossRef]
6. Shirin, V.A.; Sankar, R.; Johnson, A.P.; Gangadharappa, H.; Pramod, K. Advanced drug delivery applications of layered double hydroxide. *J. Control. Release* **2021**, *330*, 398–426. [CrossRef] [PubMed]
7. Xu, M.; Wei, M. Layered double hydroxide-based catalysts: Recent advances in preparation, structure, and applications. *Adv. Funct. Mater.* **2018**, *28*, 1802943. [CrossRef]
8. Xuan, X.; Qian, M.; Han, L.; Wan, L.; Li, Y.; Lu, T.; Pan, L.; Niu, Y.; Gong, S. In-situ growth of hollow NiCo layered double hydroxide on carbon substrate for flexible supercapacitor. *Electrochim. Acta* **2019**, *321*, 134710. [CrossRef]

9. Mohapatra, L.; Parida, K. A review on the recent progress, challenges and perspective of layered double hydroxides as promising photocatalysts. *J. Mater. Chem. A* **2016**, *4*, 10744–10766. [CrossRef]
10. Iqbal, M.A.; Fedel, M. Ordering and disordering of in situ grown MgAl-layered double hydroxide and its effect on the structural and corrosion resistance properties. *Int. J. Miner. Metall. Mater.* **2019**, *26*, 1570–1577. [CrossRef]
11. Iqbal, M.A.; Asghar, H.; Fedel, M. Double doped cerium-based superhydrophobic layered double hydroxide protective films grown on anodic aluminium surface. *J. Alloys Compd.* **2020**, *844*, 156112. [CrossRef]
12. Cao, Y.; Zheng, D.; Li, X.; Lin, J.; Wang, C.; Dong, S.; Lin, C. Enhanced corrosion resistance of superhydrophobic layered double hydroxide films with long-term stability on Al substrate. *ACS Appl. Mater. Interfaces* **2018**, *10*, 15150–15162. [CrossRef]
13. Iqbal, M.A.; Secchi, M.; Iqbal, M.A.; Montagna, M.; Zanella, C.; Fedel, M. MgAl-LDH/graphene protective film: Insight into LDH-graphene interaction. *Surf. Coat. Technol.* **2020**, *401*, 126253. [CrossRef]
14. Guo, X.; Xu, S.; Zhao, L.; Lu, W.; Zhang, F.; Evans, D.G.; Duan, X. One-step hydrothermal crystallization of a layered double hydroxide/alumina bilayer film on aluminum and its corrosion resistance properties. *Langmuir* **2009**, *25*, 9894–9897. [CrossRef] [PubMed]
15. Tedim, J.; Kuznetsova, A.I.; Salak, A.N.; Montemor, F.; Snihirova, D.; Pilz, M.; Zheludkevich, M.L.; Ferreira, M.G.S. Zn–Al layered double hydroxides as chloride nanotraps in active protective coatings. *Corros. Sci.* **2012**, *55*, 1–4. [CrossRef]
16. Zhang, L.; Gong, Z.; Jiang, B.; Sun, Y.; Chen, Z.; Gao, X.; Yang, N. Ni-Al layered double hydroxides (LDHs) coated superhydrophobic mesh with flower-like hierarchical structure for oil/water separation. *Appl. Surf. Sci.* **2019**, *490*, 145–156. [CrossRef]
17. Peng, C.; Zhang, H.; You, Z.; Xu, F.; Jiang, G.; Lv, S.; Zhang, R.; Yang, H. Preparation and anti-icing properties of a superhydrophobic silicone coating on asphalt mixture. *Constr. Build. Mater.* **2018**, *189*, 227–235. [CrossRef]
18. Li, Y.; Li, S.; Zhang, Y.; Yu, M.; Liu, J. Fabrication of superhydrophobic layered double hydroxides films with different metal cations on anodized aluminum 2198 alloy. *Mater. Lett.* **2015**, *142*, 137–140. [CrossRef]
19. Iqbal, M.A.; Asghar, H.; Fedel, M. Ce-Doped-MgAl Superhydrophobic Layered Double Hydroxide for Enhanced Corrosion Resistance Properties. *Solids* **2021**, *2*, 76–86. [CrossRef]
20. Zhang, F.; Zhao, L.; Chen, H.; Xu, S.; Evans, D.G.; Duan, X. Corrosion resistance of superhydrophobic layered double hydroxide films on aluminum. *Angew. Chem.* **2008**, *120*, 2500–2503. [CrossRef]
21. Wang, F.; Guo, Z. Facile synthesis of superhydrophobic three-metal-component layered double hydroxide films on aluminum foils for highly improved corrosion inhibition. *New J. Chem.* **2019**, *43*, 2289–2298. [CrossRef]
22. Chen, H.; Zhang, F.; Fu, S.; Duan, X. In situ microstructure control of oriented layered double hydroxide monolayer films with curved hexagonal crystals as superhydrophobic materials. *Adv. Mater.* **2006**, *18*, 3089–3093. [CrossRef]
23. Xu, F.; Wang, T.; Chen, H.; Bohling, J.; Maurice, A.M.; Wu, L.; Zhou, S. Preparation of photocatalytic TiO_2-based self-cleaning coatings for painted surface without interlayer. *Prog. Org. Coat.* **2017**, *113*, 15–24. [CrossRef]
24. Song, K.; Kim, I.; Bang, S.; Jung, J.-Y.; Nam, Y. Corrosion resistance of water repellent aluminum surfaces with various wetting morphologies. *Appl. Surf. Sci.* **2018**, *467–468*, 1046–1052. [CrossRef]
25. Zhang, Y.; Liu, J.; Li, Y.; Yu, M.; Li, S.; Xue, B. A facile approach to superhydrophobic LiAl-layered double hydroxide film on Al–Li alloy substrate. *J. Coat. Technol. Res.* **2015**, *12*, 595–601. [CrossRef]
26. Cho, D.-K.; Park, I.-K. Evolution of structural and chemical properties of CoAl-based layered double hydroxides grown on silicon substrate. *Ceram. Int.* **2018**, *44*, 8556–8561. [CrossRef]
27. Zhang, L.; Zhang, Z.; Lu, C.; Lin, J.-M. Improved chemiluminescence in fenton-like reaction via dodecylbenzene-sulfonate-intercalated layered double hydroxides. *J. Phys. Chem. C* **2012**, *116*, 14711–14716. [CrossRef]
28. Baliarsingh, N.; Parida, K.M.; Pradhan, G.C. Effects of Co, Ni, Cu, and Zn on photophysical and photocatalytic properties of carbonate intercalated MII/Cr LDHs for enhanced photodegradation of methyl orange. *Ind. Eng. Chem. Res.* **2014**, *53*, 3834–3841. [CrossRef]
29. Bai, J.; Liu, Y.; Yin, X.; Duan, H.; Ma, J. Efficient removal of nitrobenzene by Fenton-like process with Co-Fe layered double hydroxide. *Appl. Surf. Sci.* **2017**, *416*, 45–50. [CrossRef]
30. Gong, C.; Chen, F.; Yang, Q.; Luo, K.; Yao, F.; Wang, S.; Wang, X.; Wu, J.; Li, X.; Wang, D.; et al. Heterogeneous activation of peroxymonosulfate by Fe-Co layered doubled hydroxide for efficient catalytic degradation of Rhoadmine B. *Chem. Eng. J.* **2017**, *321*, 222–232. [CrossRef]
31. Yang, J.; Liu, H.; Martens, W.N.; Frost, R.L. Synthesis and characterization of cobalt hydroxide, cobalt oxyhydroxide, and cobalt oxide nanodiscs. *J. Phys. Chem. C* **2009**, *114*, 111–119. [CrossRef]
32. Greenwood, N.N.; Earnshaw, A. *Chemistry of the Elements*; Elsevier: Amsterdam, The Netherlands, 2012.
33. Wang, Y.; Zhou, X.; Yin, M.; Pu, J.; Yuan, N.; Ding, J. Superhydrophobic and Self-Healing Mg-Al Layered Double Hydroxide/Silane Composite Coatings on the Mg Alloy Surface with a Long-Term Anti-corrosion Lifetime. *Langmuir* **2021**, *37*, 8129–8138. [CrossRef]
34. Aisawa, S.; Hirahara, H.; Uchiyama, H.; Takahashi, S.; Narita, E. Synthesis and thermal decomposition of Mn–Al layered Double hydroxides. *J. Solid State Chem.* **2002**, *167*, 152–159. [CrossRef]
35. Cavani, F.; Trifirò, F.; Vaccari, A. Hydrotalcite-type anionic clays: Preparation, properties and applications. *Catal. Today* **1991**, *11*, 173–301. [CrossRef]
36. Kloprogge, J.; Frost, R.L. Fourier transform infrared and raman spectroscopic study of the local structure of Mg-, Ni-, and Co-hydrotalcites. *J. Solid State Chem.* **1999**, *146*, 506–515. [CrossRef]

37. Ni, Z.; Xia, S.; Fang, C.; Wang, L.; Hu, J. Synthesis, characterization and thermal property of Cu/Co/Mg/Al hydrotalcite like compounds. *Rare Met. Mater. Eng. S* **2008**, *2*, 634–637.
38. Wang, Z.; Shen, X.; Qian, T.; Xu, K.; Sun, Q.; Jin, C. Fabrication of superhydrophobic Mg/Al layered double hydroxide (LDH) coatings on medium density fiberboards (MDFs) with flame retardancy. *Materials* **2018**, *11*, 1113. [CrossRef] [PubMed]
39. Yan, T.; Xu, S.; Peng, Q.; Zhao, L.; Zhao, X.; Lei, X.; Zhang, F. Self-healing of layered double hydroxide film by dissolution/recrystallization for corrosion protection of aluminum. *J. Electrochem. Soc.* **2013**, *160*, C480–C486. [CrossRef]
40. Wang, L.; Zhang, K.; He, H.; Sun, W.; Zong, Q.; Liu, G. Enhanced corrosion resistance of MgAl hydrotalcite conversion coating on aluminum by chemical conversion treatment. *Surf. Coat. Technol.* **2013**, *235*, 484–488. [CrossRef]
41. Iqbal, M.A.; Fedel, M. Protective Cerium-Based Layered Double Hydroxides Thin Films Developed on Anodized AA6082. *Adv. Mater. Sci. Eng.* **2020**, *2020*, 5785393. [CrossRef]
42. Lin, K.; Luo, X.; Pan, X.; Zhang, C.; Liu, Y. Enhanced corrosion resistance of LiAl-layered double hydroxide (LDH) coating modified with a Schiff base salt on aluminum alloy by one step in-situ synthesis at low temperature. *Appl. Surf. Sci.* **2019**, *463*, 1085–1096. [CrossRef]
43. Iqbal, M.A.; Sun, L.; Asghar, H.; Fedel, M. Chlorides entrapment capability of various in-situ grown NiAl-LDHs: Structural and corrosion resistance properties. *Coatings* **2020**, *10*, 384. [CrossRef]